Multiphoton ionization of rubidium*

C. B. Collins, S. M. Curry, B. W. Johnson, M. Y. Mirza, M. A. Chellehmalzadeh, and J. A. Anderson
University of Texas at Dallas, Box 688, Richardson, Texas 75080

D. Popescu
Institute of Physics of Bucharest, Bucharest, Romania

Iovitzu Popescu
University of Bucharest, Bucharest, Romania

(Received 3 May 1976)

The multiphoton excitation of rubidium has been investigated over the 4600–6500-Å wavelength region with a tunable dye-laser source having a linewidth better than 0.1 Å and a space-charge ionization detector sensitive to a few ions per second. Multiphoton transitions have been observed to occur both through intermediate atomic states and through intermediate continuum states of the rubidium molecule. In the former case two-photon transitions have been observed from the 5^2S ground state of atomic rubidium to higher-lying n^2D levels for values of n ranging from 9 to 34 and to n^2S levels for values of n from 11 through 20. The fine-structure intervals of the n^2D levels for $n = 9$ to 13 were measured together with the line-strength ratios and were found to be in good agreement with the predictions of a simple theoretical model. At the shorter wavelengths hybrid two-photon resonances were observed to be excited through resonant intermediate continuum states of Rb_2. As a result the dispersion curve for two-photon absorption in rubidium showed what appears to be resonant intermediate $p\pi(^3\Sigma_{u1})$ and 0_g^+ terms dissociating to give a $5P_{3/2}$ atom and resulting in the strong development of features corresponding to the $5^2P_{3/2} \rightarrow n^2D_{3/2,5/2}$ part of the diffuse series, for $n \leq 50$, in absorption and the $5^2P_{3/2} \rightarrow n^2S_{1/2}$ part of the sharp series. Components to 32^2D and 30^2S were recorded to a precision of 0.3 cm^{-1} and quantum defects for these previously unobserved terms were derived. The corresponding hybrid two-photon resonances involving intermediate states dissociating to give a $5^2P_{1/2}$ atom were not observed in the wavelength interval available in this experiment.

I. INTRODUCTION

At most wavelengths the multiphoton ionization of alkali metals can be viewed as a composite of the wings of transition resonances of purely atomic or molecular character. In general, the experimentally obtained dispersion curves for such photoionization processes are highly structured and permit ready identification of the corresponding nth-order resonances of the intermediate states. In these processes n can be as large as one less than the number of photons needed to ionize the atom. From the relative strengths observed for the different resonances and from the order of their dependence on the intensity of the laser source the importance of each resonance in the total photoionization probability may be estimated for arbitrary wavelengths.

Recently the domain of this type of multiphoton spectroscopy has been enlarged through the identification of a new class of excitation resonances.[1] These are the hybrid resonances in which one transition occurs to a dissociative state of the molecules and one between resulting atomic states. The same effect that makes two-photon absorption by atoms probable also makes it likely that in actual practice both virtual and real intermediate states will be molecular in character. This is because the virtual, one-photon transitions from a ground state must be optically allowed for two-photon transitions to have an appreciable strength. For example, in the alkali metals this means that two-photon transitions from ground S states must proceed through nonresonant intermediate P states. However, since the intermediate states are optically connected to the ground state, dispersion forces between these excited atoms and neighboring ground-state atoms are resonant and hence show a long-range R^{-3} dependence. Cross sections for collisions shifting the intermediate-state energy by several laser linewidths are extremely large and suggest that intermediate states involving such polarization molecules can have major roles in multiphoton absorption processes even at relatively low atomic concentrations.

As pointed out by Collins *et al.*,[1] the inclusion of these repulsive molecular states into the scheme of multiphoton excitation and ionization of the alkali metals in the visible wavelength range represents a generalization of the three-photon models originally formulated for isolated cesium atoms.[2] In the appropriate dipole approximation for a single atom in the ground state, ψ_0, expressions for the line strength for multiphoton excitation and

ionization contain products of resonant terms of the form

$$T_1(\psi_1, \psi_0) = \langle \psi_1 | z | \psi_0 \rangle / [(E_1 - E_0) - h\nu] , \quad (1a)$$

$$T_2(\psi_2, \psi_1) = \langle \psi_2 | z | \psi_1 \rangle / [(E_2 - E_1) + (E_1 - E_2) - 2h\nu] , \quad (1b)$$

where the matrix elements are the usual dipole values with summations implied over intermediate-state quantum numbers not explicitly expressed, and the values of energy E_n correspond to the states of like subscript. Dispersion curves of processes depending on line strengths containing such terms are expected to be dominated by single-photon resonances arising from zeros in the denominator of the T_1 terms of Eq. (1a), two-photon resonances from the T_2 terms of Eq. (1b), and higher-order resonances where appropriate. Dispersion curves showing structure from such multiphoton resonances were first obtained for cesium[3,4] and, more recently, for sodium under conditions allowing for the cancellation of the Doppler width of the levels.[5-7]

For nonisolated atoms, the occurrence of molecular continuum states and polarization molecules resulting from binary collisions at large internuclear separation must be recognized. This can be done by allowing the states ψ to be molecular in character and together with the corresponding energy E to depend significantly upon internuclear separation R. This has the effect of broadening the resonance through a change in R during the lifetime of the intermediate state and of altering the selection rules determining the nonzero matrix elements. For example, the $T_1(d\pi\,^3\Pi_g, s\sigma\,^3\Sigma_u^+)$ resonance has been reported in cesium,[1] having been inferred from the detection of $T_2(n\,^2D, 6\,^2P_{3/2})$. Because of the considerable variation of the intermediate-state energy E_1 (R_1) with internuclear separation, there was the possibility of obtaining simultaneous resonances in both T_1 and T_2 terms. In particular, for those R for which

$$E_2(R=\infty) - E_1(R=\infty) = h\nu = E_1(R_1) - E_0(R_1) , \quad (2)$$

strong hybrid resonances were observed. These were energetically sharp because of the dominance of the atomic matrix element, at $R=\infty$, over molecular matrix elements appropriate for finite R during the absorption of the "second" photon. The amplitudes of these resonances were observed to be modulated in intensity by the more slowly varying T_1 term contributing the resonance on the right-hand side of Eq. (2). Such hybrid resonances resulting from the simultaneous resonance at a given wavelength of a molecular T_1 term and an atomic T_2 term considerably enlarge the multiphoton ionization probability[1,8] and provide an experimental basis for ordering the repulsive states of molecules by correlating them with dissociation limits.

This paper reports the study of the multiphoton absorption resonances observed in rubidium vapor in the 4600–6500-Å wavelength range. Both hybrid and purely atomic two-photon resonances were observed with a precision sufficient to provide new term values for atomic S and D levels with high principal quantum number. The hybrid resonances observed were fragmentary and provided a basis for locating, approximately, the several previously unobserved repulsive molecular terms reported in this work.

II. EXPERIMENTAL METHOD

The experimental method used in this and related earlier works[9,10] is based on the detection of ionization resulting from either collisional ionization or photoionization of the excited states populated by the absorption event. Useful detection sequences have been found to include direct photoionization, associative ionization, and electron-impact ionization by thermal electrons of low energy. The positive ions produced in this way enhance the output signal of a thermionic diode containing the absorbing vapor by partially neutralizing the negative space charge surrounding the heated diode filament. The relatively longer time the positive ions spend traversing the potential well of the space-charge region provides for the release of 10^4–10^6 electrons per ion from that region. This technique, when coupled with light modulation and synchronous detection, represents a modernization of the early experiments on photoionization and now forms a valuable complement to conventional absorption spectroscopy. As currently implemented, sensitivity is limited by quantum fluctuations in the diode "dark current" and is sufficient for the detection of signals as small as a few ions per second.

Details of the experimental arrangement are found in previous reports[1,4,9,10] on studies of multiphoton processes in cesium, and only the general outline of the method will be repeated here. The absorption cell itself consisted of a Pyrex glass envelope with quartz windows and an included detecting diode composed of a 0.15-mm-diam tungsten filament and a silver-disk anode, both activated with rubidium and separated by 1.5 mm. The exact position of the illuminated volume within the diode structure was not particularly critical provided the diode elements were not directly illuminated. The absorption cell was baked while being pumped to 10^{-7} Torr and subsequently filled with rubidium vapor. In operation the vapor pressure was controlled by a two-chamber oven according

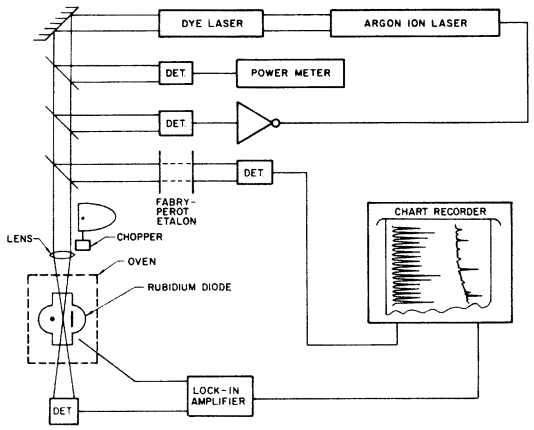

FIG. 1. Schematic representation of the arrangement of the argon-ion laser, tunable dye laser, rubidium absorption cell with included diode detector, and detection and monitoring systems used in the experiments for the detection of the purely atomic multiphoton resonances.

to standard techniques. The working pressure range corresponded to saturated vapor at 235 °C.

Two light sources were used in these experiments. In the red and yellow regions of the spectrum output from a dye laser pumped by an argon-ion laser was mechanically chopped at a frequency of 8 Hz and focused into the absorption cell, as shown in Fig. 1. Wavelength tuning and linewidth were continuously monitored with an etalon of variable spacing. As shown, the intensity passing the etalon was recorded on one channel of a two-channel recorder and the suitably conditioned diode output was recorded on the other. In this system linewidths were found to be of the order of 0.25 Å.

In the green and blue wavelength regions containing the hybrid resonances a pulsed dye laser pumped by a nitrogen laser was used as the absorption source. Pulse widths were of the order of 10 nsec and repetition rates were 8 sec^{-1}, as limited by the characteristic drift time for ions in the space charge region of the detecting diode. The dye laser was operated with either acidified 4-methylumbelliferone or with a mixture of disodium fluorescein and coumarin-1 and was continuously tuned with better than 0.1 Å linewidth. In this pulsed system the laser output was not constant as a function of either time or wavelength, and for maximum sensitivity it was found necesary to simultaneously convert to digital form both the diode output signal resulting from the photoabsorptions and the input laser intensity for each pulse. This was accomplished with a 10-bit A/D conversion system directly interfaced to an instrumentation computer, as discussed previously.[4]

In operation either laser source was sufficient to excite multiphoton resonances lying in the appropriate wavelength range. These resonances could be detected from the substantial increase in photoionization current from the diode observed at certain laser wavelengths, which could be determined interferometrically. Resulting system resolution was better than 0.3 cm^{-1}, so that atomic term values of newly observed levels could be determined to at least this precision.

III. RESULTS AND CONCLUSIONS

A. Purely atomic resonances, $5^2S \rightarrow n^2S$ and $5^2S \rightarrow n^2D$

With the cw dye laser system the purely atomic, two-photon resonances of rubidium were excited in the 5700–6300-Å wavelength region. Figure 2 shows typical data obtained. Components of the $5^2S \rightarrow n^2D$ and $5^2S \rightarrow n^2S$ two-photon Rydberg series are marked in the figure. The more pronounced lines correspond to members of the $T_2(5^2D \rightarrow n^2F)$ hybrid resonances of the cesium which was present as an impurity at the beginning of the life of the diode detector. Studies of the same spectrum observed in pure cesium have been previously reported[1] and comprised the first observation of a hydrid multiphoton resonance. In the work reported here the trace amounts of cesium gradually disappeared as the diode aged, most probably through reactions with the metallic electrodes and quartz windows. At shorter wavelengths than those shown in Fig. 2 higher members of the two-photon Rydberg series of rubidium were excited. Over the full wavelength range examined, transitions from $n = 9$–34 were observed for the $5^2S \rightarrow n^2D$ series and from $n = 11$–20 for the $5^2S \rightarrow n^2S$ series.

A higher resolution of the recorded signal was obtained by scanning the wavelength more slowly,

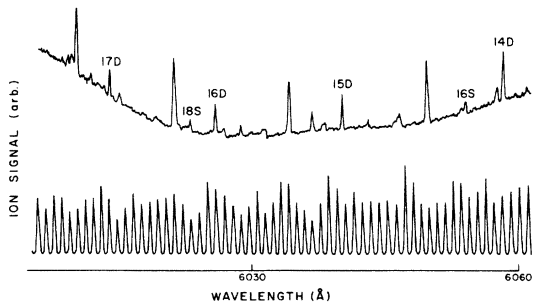

FIG. 2. Upper curve: dispersion curve of the photoionization current detected from the rubidium diode as a function of wavelength. Components of the $5^2S \rightarrow n\,^2D$ and $5^2S \rightarrow n\,^2S$ two-photon Rydberg series are marked with the appropriate value of n. The more pronounced unmarked lines correspond to the excitation of hybrid resonances of cesium which was present as an impurity. Lower curve: detected laser intensity filtered by the Fabry-Perot etalon used for wavelength measurements.

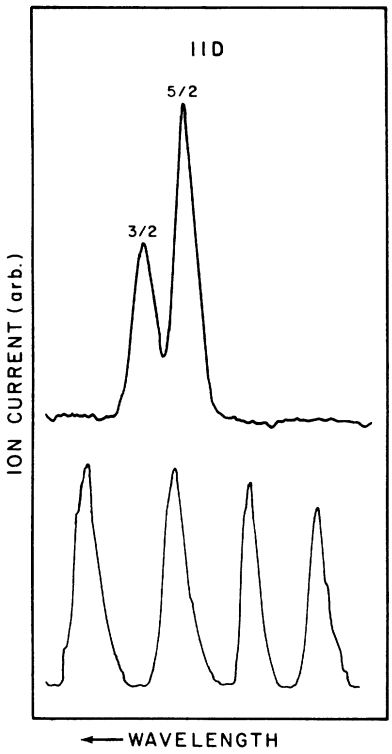

FIG. 3. Upper curve: dispersion curve of the photoionization current detected from the rubidium diode as a function of wavelength for the interval near 6149.3 Å. The resolved fine-structure splitting of the $5\,^2S \rightarrow 11\,^2D$ component of the two-photon Rydberg series is shown. Lower curve: detected laser intensity filtered by the 1.2981-cm air-spaced Fabry-Perot etalon used for calibration.

and Fig. 3 shows typical data obtained. In this figure the $5\,^2S \rightarrow 11\,^2D$ doublet is shown with resolution sufficient to determine the fine-structure splitting of the D state. Comparison of the photoionization peaks recorded to the positions of the transmission maxima of the 1.2981-cm air-spaced etalon according to standard techniques[11] allowed for the determination of the fine-structure splitting of the $n\,^2D$ states to $n = 13$.

Although fine-structure intervals are reported for D states by Moore[12] to the same value of n, the values reported here are in better agreement with the Landé formula,

$$\Delta E = [\alpha^2 Z_a^2 Z_i^2 / l(l+1)\sqrt{R_\infty}]E^{3/2}\ \text{cm}^{-1}, \qquad (3)$$

where ΔE and E are the energies in cm^{-1} of the splitting and ionization energy, respectively, Z_i and Z_a are the effective inner and outer Z values, R_∞ is the Rydberg constant, l is the orbital angular momentum quantum number, and α is the fine-structure constant. Figure 4 shows this agreement between the present data and the Landé formula represented in this case by the "best" straight-line fitting to the data when plotted as a function of the $\frac{3}{2}$ power of the ionization energy. The tabulated data of Moore are also shown for comparison. If the values of effective charge appearing in (3) are completely independent of principal quantum number, then the slope of the best linear fit to the data should be 1. The line seen in Fig. 4, however, was found to have a slope of 1.02, which means that

$$\Delta E \propto E^{1.53}. \qquad (4)$$

Assuming then that $Z_a = 1$, the appropriate value of inner charge can be computed from the proportionality constant of Eq. (4) and the data of Fig. 3 to vary from $Z_i = 17.68$ for $9\,^2D$ to $Z_i = 17.55$ for $13\,^2D$.

From data such as those of Fig. 3 an important comparison of observed line-strength ratios can be made with theory. While the overall calibration of the detection efficiency of the space-charge diode has not been made because of the difficulty of correctly estimating the focal volume of the laser radiation, relative measurements should be significant over sufficiently restricted tuning ranges. It has been shown by Curry *et al.*[13] that the line-strength ratio of two photon doublets can be reasonably approximated by the expression

$$R = 54/(1+5r)^2, \qquad (5)$$

where R is the line-strength intensity ratio, $R = I(\frac{5}{2})/I(\frac{3}{2})$, and r is the ratio of the energy defects appearing in the denominators of the $T_1(5\,^2P_{3/2}, 5\,^2S)$

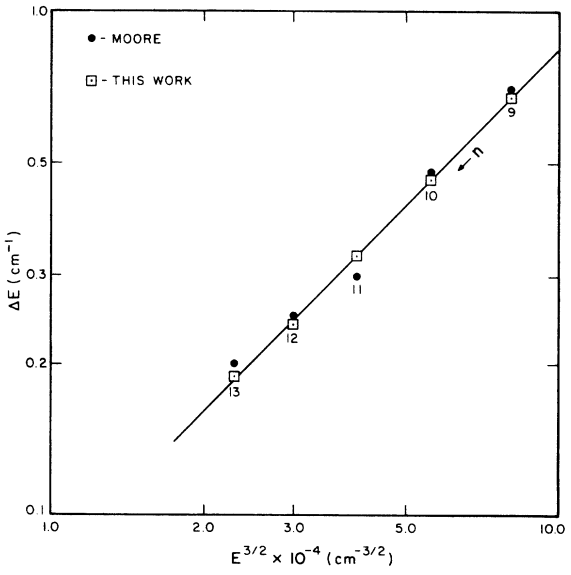

FIG. 4. Comparison of measurements of the fine-structure splitting of the $n\,^2D$ levels of rubidium with the Landé theory and the previous data tabulated by Moore. Data are plotted as functions of the ionization energy, in cm^{-1}, raised to the $\frac{3}{2}$ power.

TABLE I. Comparison of the line-strength ratios for the intensities of the two-photon $5\,^2S \rightarrow n\,^2D$ doublets observed in this work with the theoretical estimate given by Eq. (5) for $n = 9$–13.

Principal quantum number n	Ratio Calculated	Observed
9	1.695	1.65
10	1.683	1.77
11	1.675	1.76
12	1.670	1.84
13	1.666	2.0

and $T_1(5\,^2P_{1/2}, 5\,^2S)$ resonance terms. For example, for the $11\,^2D$ level the photon energy $h\nu$ is 16 257.39 cm^{-1}, giving the energy denominators for excitation through nonresonant $5\,^2P_{3/2}$ and $5\,^2P_{1/2}$ level values of 3440.83 and 3678.43 cm^{-1}, respectively. The corresponding value of r is then 0.935, giving an expected line strength ratio of 1.68, in good agreement with the ratio of 1.76 actually observed. Results of a comparison of line-strength ratios observed in this work to those computed from Eq. (5) are summarized in Table I.

The divergence of computed and observed values at higher n is most probably due to a breakdown of the rather severe approximations used in simplifying the theoretical estimate. In particular, it was assumed that only two intermediate states, $5P_{1/2}$ and $5P_{3/2}$, were important, and hence that the transition strength contained only the two T_1 resonances, $T_1(5P_{3/2}, 5S)$ and $T_1(5P_{1/2}, 5S)$, and furthermore that the radial parts of these two resonances were identical. That these are reasonable but not exact approximations is seen from Table I.

Although new term values for the higher $n\,^2S$ levels were obtained from this work, the same levels were more strongly excited as the result of hybrid resonances, as discussed in Sec. III B, and it was from those spectra that new term values were taken. Rather, an examination of ionization yield as a function of laser intensity was made as a final confirmation of the nature of the excitation sequence. Figure 5 presents the data obtained, and a strong second-order dependence can be seen. This is consistent with the lower laser intensity employed since it is only in the higher-power pulsed laser experiments that photoionization of the excited states produced by the multiphoton absorption can compete with collisional ionization. The most probable detection sequence appropriate to the cw excitation is

$$\mathrm{Rb}(5\,^2S) + 2h\nu \rightarrow \mathrm{Rb}^*(n\,^2S \text{ or } n\,^2D), \tag{6a}$$

followed by

$$\mathrm{Rb}^* + \mathrm{Rb} \rightarrow \mathrm{Rb}_2{}^+ + e^- \tag{6b}$$

or by

$$\mathrm{Rb}^* + \mathrm{Rb} \rightarrow \mathrm{Rb}^+ + \mathrm{Rb}^-, \tag{6c}$$

with the quadratic dependence of output upon laser intensity being a consequence of step (6a).

B. Hybrid two-photon resonances

As discussed above, the pulsed dye laser system was used to investigate the green and blue regions of the rubidium spectrum. Most pronounced in this wavelength region was found to be the strong development of structure corresponding to fragments of the diffuse series of atomic rubidium. However, only components of the $5\,^2P_{3/2} \rightarrow n\,^2D_{5/2,3/2}$ series were found, with the analogous resonances from the $5\,^2P_{1/2}$ level being completely absent. These resonances from the $5\,^2P_{3/2}$ level were found to be strongly developed, together with the underlying structure from the "blue bands" of the Rb_2 molecule[14] resulting from two-photon ionization of Rb_2 through the resonant intermediate B state of the molecule. This is entirely analogous to the two-photon ionization of Cs_2 found previously[10] in diodes containing cesium vapor.

The resulting ion current corresponding to the

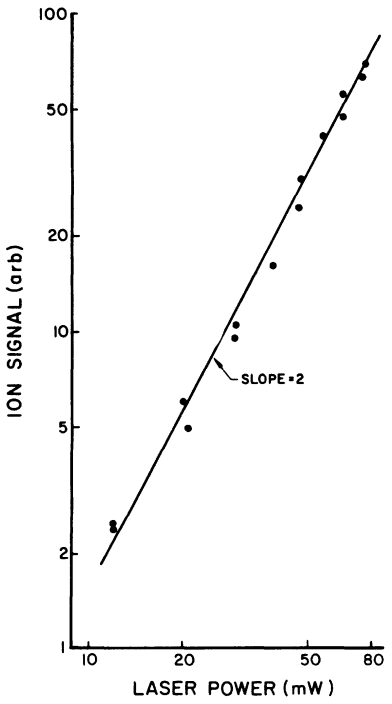

FIG. 5. Photoionization current less dark current as a function of cw dye laser intensity for the $5\,^2S \rightarrow 15\,^2D$ transition at 6040.2 Å. A line of slope 2 has been shown for comparison.

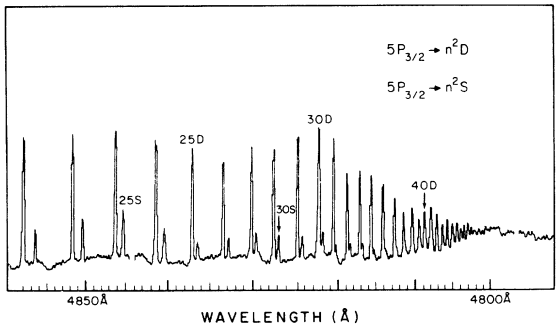

FIG. 6. Multiphoton absorption spectrum of rubidium as a function of wavelength, showing hybrid resonances corresponding to parts of the diffuse ($5\,^2P_{3/2} \rightarrow n\,^2D$) and sharp ($5\,^2P_{3/2} \rightarrow n\,^2S$) series of atomic rubidium. No resonances involving the $5\,^2P_{1/2}$ level are observed. Data plotted are the ion signals from the rubidium diode divided by the square of the simultaneously measured laser intensities. Irregularities seen in the wavelength scale are artifacts from the drive mechanism and have been calibrated as shown.

relative probability of two-photon absorption in rubidium is shown as a function of wavelength in Fig. 6. The data plotted are the outputs from the on-line computer system and represent the detected ion signals divided by the square of the simultaneously measured laser intensities. The *a priori* appearance of a Rydberg series of doublets is misleading since the spectrum is actually a composite of the individual sharp ($5\,^2P_{3/2} \rightarrow n\,^2S_{1/2}$) and diffuse ($5\,^2P_{3/2} \rightarrow n\,^2D$) series, with the true doublets of the latter being unresolved. Members of the diffuse series can be clearly identified to $50\,^2D$ and those of the sharp series to $36\,^2S$. Term values have not been previously reported for S levels of such large n. From data such as those of Fig. 6 taken simultaneously with the spectrum of the transmission maxima of a 1.78 757-mm air-spaced etalon new term values were obtained for D states to $30\,^2D$ and S states to $32\,^2S$. These are summarized in Table II. Precision is estimated to be better than 0.3 cm^{-1}. Finally, from such data the quantum defects of the D and S levels can be readily obtained and these are shown in Figs. 7 (a) and 7(b).

TABLE II. Term values in cm^{-1} for the $n\,^2D$ and $n\,^2S$ levels obtained from the hybrid resonances excited in this experiment.

n	$n\,^2D$	$n\,^2S$
14	33 005.6	
15	33 102.2	
16	33 179.9	33 027.9
17	33 243.0	33 119.9
18	33 295.5	33 194.3
19	33 339.0	33 255.1
20	33 375.5	33 305.2
21	33 406.9	33 347.2
22	33 433.6	33 382.4
23	33 456.7	33 413.1
24	33 477.1	33 438.9
25	33 494.5	33 461.0
26	33 510.2	33 480.9
27	33 524.2	33 498.1
28	33 536.6	33 513.5
29	33 547.5	33 526.8
30	33 557.3	33 539.2
31		33 549.7
32		33 559.0

The nonoccurrence of transitions from the $5\,^2P_{1/2}$ level is the strongest argument in support of the basic assumption of this work, that the transitions observed are excited as integral parts of a two-photon process. This must be expected from the fact that the duration of the laser pulse is about four orders of magnitude less than the inverse collision frequency and effectively precludes any appreciable excitation transfer between rubidium atoms during the time the diffuse series could be excited. Similarly, the repetition rate of the laser is orders of magnitude slower than the destruction

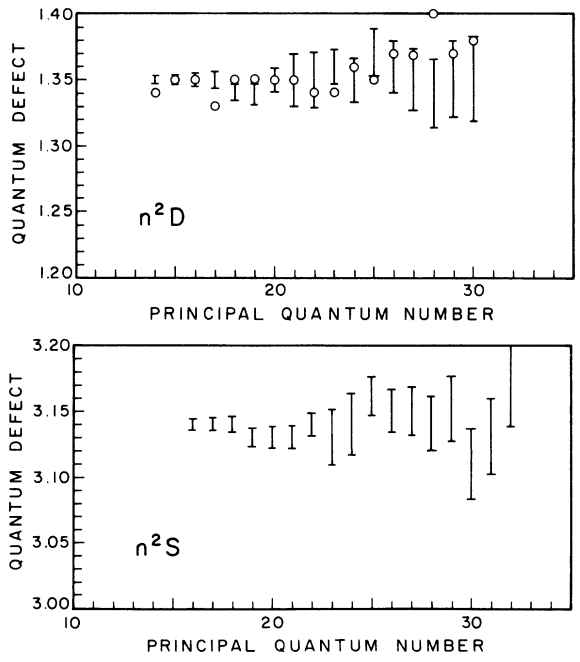

FIG. 7. Plot of the quantum defects of the Rydberg levels of atomic rubidium inferred from the hybrid two-photon resonances corresponding to the sharp and diffuse series in absorption. Upper curve: quantum defects of the $n\,^2D$ levels measured in this work are bounded by the error bars shown, open circles plot values derived from Ref. 12. Lower curve: quantum defects observed in this work for the $n\,^2S$ levels.

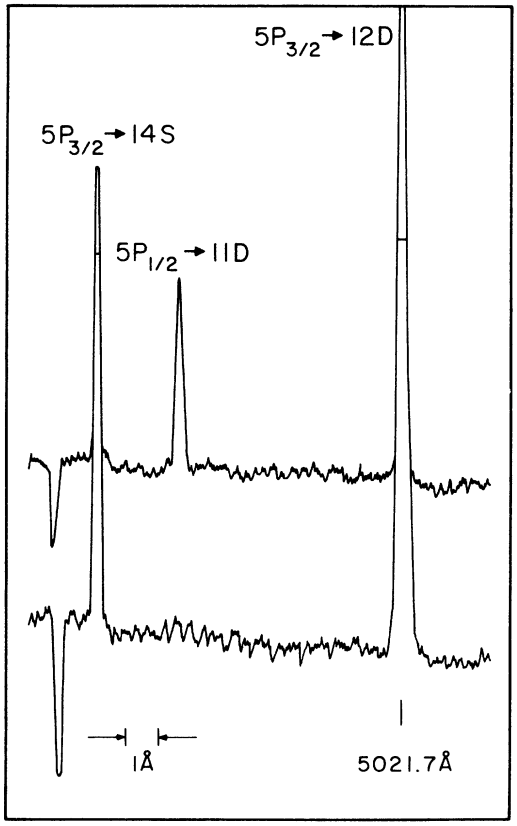

FIG. 8. Relative photoionization current detected from the rubidium diode plotted as a function of wavelength. Resonances corresponding to components of the diffuse and sharp series of atomic rubidium are identified. Upper curve: data obtained from the absorption of the pulsed laser radiation in the vapor illuminated with an auxiliary continuous source of collimated but unfocused radiation filtered with a red filter. Lower curve: comparison data to that of the upper curve obtained under the same conditions but without the auxiliary illumination of the vapor.

frequency for excited species produced by preceding pulses, so that the production of $5\,^2P_{3/2}$ atoms and the subsequent transition to the $n\,^2D$ or $n\,^2S$ states must occur within the same 10^{-8} sec interval. The converse circumstance is illustrated by the auxiliary illumination of the vapor cell with collimated but unfocused illumination from a continuous source, in this case a slide projector filtered with a red filter. This permitted the continuous excitation of both $5\,^2P_{3/2}$ and $5\,^2P_{1/2}$ through absorption of the resonance lines by the ground-state atoms and was expected to result in the excitation by the laser pulse of the diffuse and sharp spectral series from both P states. The results from such a mixture of continuous and pulsed illumination are shown in Fig. 8, together with the corresponding data for purely pulsed illumination. It can be clearly seen that the auxiliary cw illumination supported the excitation in this wavelength segment of the $5\,^2P_{1/2} \rightarrow 11\,^2D$ transition, while in the data of the lower trace, obtained with only the laser excitation, it was completely absent. All of the transitions of the diffuse and sharp series were found to follow this pattern, and no resonance corresponding to a transition from $5\,^2P_{1/2}$ could be found without supplementary illumination at long wavelengths.

The most probable explanation of the nonoccurrence of the $5\,^2P_{1/2}$ transitions is that the resonances observed do indeed represent hybrid resonances and that the T_1 resonances between molecular levels dissociating to give a $5\,^2P_{1/2}$ atom do not occur at wavelengths corresponding to components of the diffuse series in absorption. This, then, precludes T_2 resonances being excited at these same wavelengths.

Unfortunately, little is known about the possible, but previously unobserved, repulsive states of Rb_2. Both Mulliken[15] and Fontana[16,17] have estimated the potential curves for such states at large R, but no information has been available for values of R characteristic of optical transitions. The appearance and nonappearance of hybrid resonances involving the $5\,^2P_{3/2}$ and $5\,^2P_{1/2}$ states, respectively, provide the information needed to resolve previous ambiguities in the correlation of the possible repulsive molecular terms with their dissociation limits. As seen below, relatively straightforward assumptions now yield a first approximation to the repulsive potential curves of the Rb_2 system.

Both $^1\Sigma_g^+$ and $^3\Sigma_u^+$ states can arise from the collision of two $5\,^2S_{1/2}$ ground-state atoms. The former is strongly bound and forms the ground state of the Rb_2 molecule with a dissociation energy[18] of 3952 cm^{-1}. The triplet state is repulsive, with a small Van der Waals minimum[18] of a few tens of cm^{-1} around 7.2 Å. Depending upon the height of possible centrifugal barriers, equilibrium populations of both states could be expected to be of the order of 10^3–10^5 cm^{-3} for energies within a few kT of that of an isolated $5\,^2S$ atom at a pressure of 0.1 Torr.

Thus transitions of the T_1 type could occur for three possible populations and internuclear separations: (a) the strongly bound Rb_2 population of the $^1\Sigma_g^+$ state around 4.1 Å; (b) the population of the vibrationally excited levels of the $^1\Sigma_g^+$ state within a few kT of the dissociation limit at internuclear separations corresponding either to the inner turning point at $R < 4$ Å or to the outer at large values of R; and, finally (c) the population of the $^3\Sigma_u^+$ Van der Waals state at $R \geq 6$ Å for collision energies less than $2kT$. Considering that a T_1 transition for $\lambda \sim 5000$ Å involving one of these must give a $5\,^2P_{3/2}$

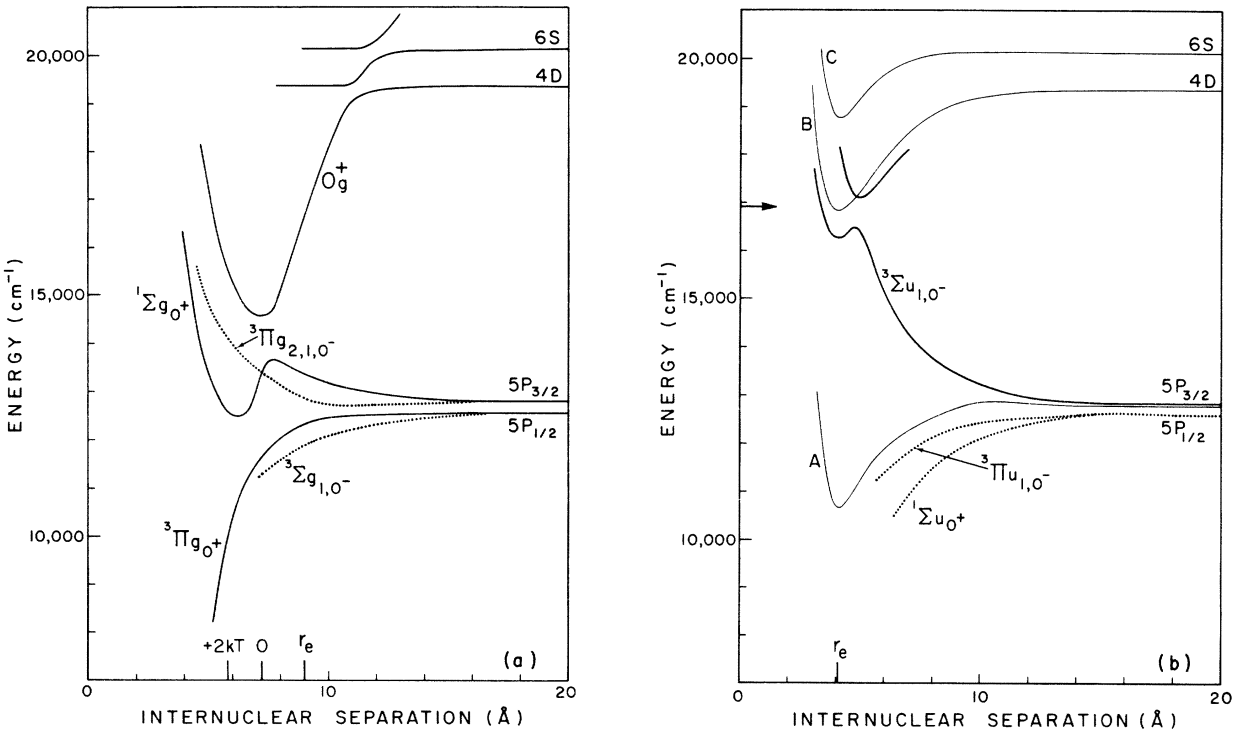

FIG. 9. Potential curves as functions of internuclear separation in Å for the energy in cm^{-1} of Rb* + Rb above the energy of an isolated $5\,^2S$ atom. Curves are drawn to be consistent with previous theoretical calculations, the principle of avoided crossings, and the hybrid resonances observed in this work. Heavy lines plot potentials which are indicated to be important in formation of hybrid resonances, light curves show bound states known from conventional spectroscopy, and dotted curves represent states, shown for completeness, which might contribute to hybrid resonances at wavelengths longer than those used in these experiments. (a) Potential curves for selected excited states of g symmetry. Indicated on the abscissa are internuclear separations corresponding to the potential minimum, zero energy, and potential equal to twice the thermal energy for the lowest $^3\Sigma_u$ state resulting from two ground-state atoms. (b) Potential curves for selected excited states of u symmetry. Indicated on the abscissa is the equilibrium internuclear separation of the ground $^1\Sigma_g$ state of Rb_2. Energy typical of that needed to excite the T_1 resonance leading to subsequent excitation of the highest-lying $n\,^2D$ states is shown by an arrow on the ordinate.

atom and that no T_1 transition at this wavelength can give a $5\,^2P_{1/2}$ atom greatly assists in the ordering of the 16 possible molecular terms dissociating to give a $5\,^2P$ atom.

A first approximation to the system of potential curves for the lower electronically excited states of Rb_2 can be constructed from the following five bases: (i) The known fine-structure splitting of the $5\,^2P$ atomic levels; (ii) the resonant R^{-3} dispersion forces given by Fontana[16,17]; (iii) avoided crossings with the 0_g^+ state of the ionic molecule, $Rb^+ + Rb^-$, using an electron affinity[19] of 0.486 eV; (iv) the fact that the longest-wavelength absorption band of Rb_2 is correctly identified in the literature[20] as a $\Sigma \rightarrow \Pi$ transition; and (v) the hybrid resonances observed in this work.

Figure 9 shows the resulting construction separately for u and g states, emphasizing levels of importance in the visible wavelength region. Considering first the g states, it should be noted that because of the strongly repulsive nature of the lower $^3\Sigma_u$ states, transitions must occur at $R > 6$ Å unless very high temperatures are assumed. Transitions at smaller R from the $^1\Sigma_g$ state are forbidden by the $u \rightarrow g$ selection rule. Clearly, then, transitions at wavelengths shorter than 5167 Å, or energies greater than the excitation energy of a $4\,^2D$ state from a $5\,^2S$ ground state of the atom, can result only in the excitation of a molecular g state dissociating to a $4\,^2D$ or higher-energy state of the atom and so cannot account for the observed excitation of the diffuse series. Conversely, at lower energies, for wavelengths between 5167 and 6900 Å, vibrational overlap integrals should favor transitions from the $^3\Sigma_{u1}$ state to the deeply bound 0_g^+ state formed by an avoided crossing of the $^1\Sigma_{g0^+}$ state arising from $(5\,^2P_{3/2} + 5\,^2S_{1/2})$ and the 0_g^+ state of the ionic molecule. That this crossing is avoided only in the adiabatic approximation suggests that for high vibrational energies, such as those favored by a

vertical transition to this state from the minimum of the $^3\Sigma_u^+$ Van der Waals state, a considerable predissociation could be expected through the crossing to give a $5\,^2P_{3/2}$ atom. This could easily contribute the T_1 resonance needed to explain the occurrence of the transitions from the $5\,^2P_{3/2}$ level, at least for $\lambda > 5167$ Å. This wavelength range, however, does not include T_2 resonances at shorter wavelengths reaching to the limit of the diffuse series. The other possible g states of Rb_2 dissociating to $5\,^2P$ can be eliminated, since they lie too low to contribute T_1 resonances for the excitation of either $5\,^2P_{3/2}$ or $5\,^2P_{1/2}$ states in the visible wavelength range.

Considering, then, the molecular u states, the range of internuclear separations of interest includes smaller values. Although valence-type forces lying outside the scope of these approximations may modify a curve sufficiently to bring it into the region of importance, the state of most probable interest is the $^3\Sigma_{u1}$. This is the state with the most strongly repulsive dispersion force, and it has been drawn to conform to the calculation of Fontana.[16] The three bound states known from conventional spectroscopy[14,20] have been included for comparison. It can be seen that at 5 Å the repulsive energy of the dispersion forces is sufficient to bring the $^3\Sigma_u$ state originating from $(5\,^2P_{3/2} + 5\,^2S_{1/2})$ into the region where the bound states which dissociate into a $4\,^2D$ atom would lie. It is highly probable that in this region a 1_u attractive curve resulting from $(4\,^2D + 5\,^2S)$ would be encountered and an avoided crossing would result in the form of the potential curve shown. A second bound 1_u curve should also be formed, but displaced to larger equilibrium internuclear separations, so that a conventional absorption spectrum to that level may have remained unobserved because of unfavorable overlap integrals.

The only other state optically connected to the $^1\Sigma_g$ ground state and having a repulsive resonant dispersion force is the other 1_u state originating from $5\,^2P_{3/2}$, but this must correlate with $^1\Pi_u$ and hence be attractive if the original assignment[20] of the $X \rightarrow A$ absorption band is correct. If it is not correct and the transition is a $\Sigma \rightarrow \Sigma$, as is the case in the lighter alkali metals, then the $^1\Pi_u$ state can provide the strongly repulsive curve which is sought to explain the hybrid resonances. In either case the only remaining 1_u curve available to $(5\,^2P_{1/2} + 5\,^2S)$, as well as the 0_u^+ curve, must lie at energies too low to contribute T_1 resonances in the visible region in order to avoid crossing levels with similar Ω arising from $(5\,^2P_{3/2} + 5\,^2S)$.

Consequently, it appears that the arrow shown in the u system of the molecule must represent the T_1 resonance at the shorter wavelengths corresponding to the limit of the diffuse series. Collecting the results from u and g systems we note that it appears that the hybrid resonances observed in this work can be best described for visible wavelengths $\lambda > 4800$ Å by the sequences

$$Rb_2(^1\Sigma_g) + h\nu \rightarrow Rb_2{}^{**}(^3\Sigma_{u1}), \tag{7a}$$

$$Rb_2{}^{**}(^3\Sigma_{u1}) \rightarrow Rb + Rb^*(5\,^2P_{3/2}), \tag{7b}$$

and for visible wavelengths $5150 < \lambda < 6900$ Å,

$$Rb_2(^3\Sigma_u) + h\nu \rightarrow Rb_2{}^{**}(0_g^+), \tag{8a}$$

$$Rb_2{}^{**}(0_g^+) \rightarrow Rb + Rb^*(5\,^2P_{3/2}), \tag{8b}$$

where the double asterisk indicates a state unstable against dissociation or predissociation. These T_1 resonances would then be followed by absorption of a second photon if its energy also corresponded with a possible T_2 resonance of the diffuse or sharp series in absorption. The final ionization would be accomplished by either step (6b) or (6c). As can be seen from Fig. 9, no potential curves which dissociate to $5P_{1/2}$ are available to give T_1 resonances in the visible wavelength range, in agreement with the absence of observed diffuse series components corresponding to the excitation of $5\,^2P_{1/2}$ intermediate states.

IV. SUMMARY

While it has been shown that the purely atomic, two-photon absorption resonances observed in the photoionization of atomic rubidium do conform to the theoretical expectations, both in fine structure and line-strength ratios, even stronger hybrid resonances have been demonstrated. Because of the greater intensity observed for such hybrid resonances, they are shown to compete favorably with the purely atomic, two-photon absorption spectra in the determination of spectroscopic constants of levels which are difficult to excite by the conventional techniques of spectroscopy.

Hybrid resonances, being partly molecular and partly atomic, can be expected to contribute heavily to the multiphoton ionization cross section at shorter wavelengths for rubidium vapor at moderate density. However, not only do such resonances contribute to the enlargement of ion yields obtained at given laser intensities, but also, as demonstrated in this work, they provide an important mechanism for the ordering and correlation of repulsive molecular terms with their dissociation limits.

*Conducted as part of the U. S.-Romanian Cooperative Program in Science and Technology between the University of Texas at Dallas and the Institute of Physics and University of Bucharest. Support was provided in part by NSF Grant No. GF 443 and in part by the Romanian CSEN and CNST.

[1]C. B. Collins, B. W. Johnson, M. Y. Mirza, D. Popescu, and I. Popescu, Phys. Rev. A 10, 813 (1974).
[2]H. B. Bebb, Phys. Rev. 153, 23 (1967).
[3]B. Held, G. Mainfray, C. Manus, J. Morellec, and F. Sanchez, Phys. Rev. Lett. 30, 423 (1973).
[4]D. Popescu, C. B. Collins, B. W. Johnson, and I. Popescu, Phys. Rev. A 9, 1182 (1974).
[5]F. Biraben, B. Cagnac, and G. Grynberg, Phys. Rev. Lett. 32, 643 (1974).
[6]M. D. Levenson and N. Bloembergen, Phys. Rev. Lett. 32, 645 (1974).
[7]T. W. Hänsch, K. C. Harvey, G. Meisel, and A. L. Schawlow, Opt. Commun. 11, 50 (1974).
[8]M. LuVan, G. Mainfray, C. Manus, and I. Tugov, Phys. Rev. A 7, 91 (1973).
[9]D. Popescu, M. L. Pascu, C. B. Collins, B. W. Johnson, and I. Popescu, Phys. Rev. A 8, 1666 (1973).
[10]C. B. Collins, B. W. Johnson, D. Popescu, G. Musa, M. L. Pascu, and I. Popescu, Phys. Rev. A 8, 2197 (1973).
[11]R. S. Longhurst, *Geometrical and Physical Optics*, (Longmans, Green, New York, 1957), p. 162.
[12]C. E. Moore, *Atomic Energy Levels*, Natl. Bur. Stand. (U. S. GPO, Washington, D. C., 1958), Vol. II, p. 180.
[13]S. M. Curry, C. B. Collins, M. Y. Mirza, D. Popescu, and I. Popescu, Opt. Commun. 16, 251 (1976).
[14]N. T. Ze and T. San-Tsiang, Phys. Rev. 52, 91 (1937).
[15]R. S. Mulliken, Phys. Rev. 120, 1674 (1960).
[16]P. R. Fontana, Phys. Rev. 123, 1871 (1961).
[17]P. R. Fontana, Phys. Rev. 125, 1597 (1962).
[18]H. O. Dickinson and M. R. Rudge, J. Phys. B 3, 1448 (1970).
[19]A. Kasdan and W. C. Lineberger, Phys. Rev. A 10, 1658 (1974).
[20]P. Kusch, Phys. Rev. 49, 218 (1936).